Electrospun Nanoparticle–Nanofiber Composites via a One-Step Synthesis

*Carl D. Saquing, Joshua L. Manasco, and Saad A. Khan**

***A** facile approach to synthesize and incorporate metal nanoparticles (NPs) into electrospun polymer nanofibers (NFs) wherein the electrospinning polymer acts as both a reducing agent for the metal salt precursor, as well as a protecting and templating agent for the ensuing NPs, is reported. Such a true one-step process at ambient conditions and free of organic solvents is demonstrated using a system comprising $AgNO_3$ and poly(ethylene oxide) (PEO) at electrospinnable molecular weights of 600, 1000, or 2000 kDa. The PEO transforms Ag^+ into AgNPs, a phenomenon that has not been previously possible at PEO molecular weights less than 20 kDa without the addition of a separate reducing agent and stabilizer or the application of heat. Results from X-ray photoelectron spectroscopy and UV–Vis absorption spectrophotometry analyses support the formation of pseudo-crown ethers in high molecular weight PEO as the mechanism in the development of NPs. The AgNPs reduce fiber diameter and enhance fiber quality (reduced beading) due to increased electrical conductivity. Interestingly, several of the NFs exhibit AgNP-localized nanochain formation and protrusion from the NF surface that can be attributed to the combined effect of applied electrical field on the polymer and the differences between the electrical conductivity and polarizability of the polymer and metal NPs.*

Keywords:
- electrospinning
- nanofibers
- nanoparticles
- one-step synthesis
- silver

1. Introduction

The synthesis of nanoscale composite materials has attracted a great deal of attention due largely to their unique physical and chemical properties at this length scale.[1–5] Metal nanoparticles (NPs) of uniform and controllable size and composition contained in an appropriate substrate find relevance in areas as diverse as catalysis, microelectronics, medicine, sensing, magnetics, electrochemistry, and optics.[6–10] The special properties exhibited by these materials in such applications depend strongly on the size, spatial distribution, and specific concentration of the metal clusters incorporated in the host matrix.[1,6,9] Hence, the incorporation of metal NPs on the surface of fibers presents the opportunity to design high-performance functional fabrics based on electrospinning (ES) for applications that include catalysis, sensors, and medical and packaging devices containing antimicrobial elements.

To date, the few studies that have incorporated noble metals (e.g., Au and Ag) in polymers via ES have used procedures that involved several steps and a separate reduction of the metal ion with a reducing agent and/or the addition of a stabilizer or protecting agent.[11–14] Most of these earlier methods can be classified into two general categories. In one category, the NPs are prepared using established chemical reduction methods[15,16] where the aqueous metal salt solution and a strong, usually toxic, reductant (e.g., $NaBH_4$ in $[CH_3(CH_2)_7]_4NBr$) dissolved in an organic solvent (e.g. toluene) are mixed and then the NPs are subsequently extracted with a non-water-soluble capping/stabilizing agent.[11] The extracted NPs are added to the polymer dissolved in

[*] Prof. S. A. Khan, Dr. C. D. Saquing, J. L. Manasco
Department of Chemical and Biomolecular Engineering North Carolina State University
Raleigh, NC 27695-7905 (USA)
E-mail: khan@eos.ncsu.edu

DOI: 10.1002/smll.200801273

NANO MICRO small

chloroform and electrospun. In the other category, the metal salt is added to the polymer solution, electrospun, and the resulting nanofiber (NF) mat is subjected either to a thermal,[17,18] radiolytic (e.g., UV),[19] chemical treatment process[20,21] or a combination of heat and chemical treatment processes[14] to reduce the metal ions.

In this paper, we describe for the first time the use of an ES polymer that acts as both the reducing agent for the metal salt precursor and the protecting agent for the resulting metal NPs in solution. The subsequent ES of the solution also facilitates the use of the ES polymer as a template to fabricate polymer NF–NP composites. Poly(ethylene oxide) (PEO) is used as a model system to demonstrate this unique procedure, although in principle other polymers may also be utilized as long as they are able to reduce the metal NP precursor and to be electrospun. One of the challenges in AgNP synthesis is the extreme difficulty of finding an appropriate solid support to which Ag^+ can be reduced to Ag^0 at ambient temperature.[22] In only a handful of studies, poly(vinyl pyrollidone) (PVP), through its hydroxyl terminating endgroups, has been shown to deoxidize Ag^+ to form NPs with various sizes in aqueous solution.[10,23,24] This has, however, been achieved only upon heating, and no fibers have been developed. Low molecular weight (MW) PEO has been shown to transform Au complexes (using $NaAuCl_4 \cdot 2H_2O$ and $HAuCl_4 \cdot 3H_2O$ as precursors) into their corresponding AuNPs in an aqueous system at ambient conditions presumably through the formation of pseudo-crown ethers by PEO.[25,26] However, in the case of Ag complexes (e.g., using $AgNO_3$), the reduction by low MW PEO has been slow, requiring at least 20 days.[25]

We hypothesize that with high MW PEO (such as 600 to 2000 kDa), metal salts can be reduced at shorter times and under ambient conditions (due to increased reaction sites) and still allow the electrospinning of the resulting PEO–NP system. If successful, this would allow the development of a one-step and environmentally benign methodology, hence sustainable, for the synthesis of NPs and NP–NF composites involving ES. We show that, for the $AgNO_3$–PEO system, this is the case.

Additional advantages of the use of PEO are its biocompatibility and its wide use[27] as a biomaterial for scaffolds,[28] drug delivery,[29,30] tissue engineering, wound healing,[31] and conductive fibers for electrolytes in polymer batteries.[32,33] Since PEO features amphiphilic properties, it is easily amenable for combination with other polymers, either chemically or physically; its characteristics can be tailored to suit a particular application. The system has the potential to be a building block for fabricating polymer–metal NP nanocomposites. Moreover, its solubility in water and in several polar and nonpolar organic solvents makes it an excellent model polymer–NP system for gaining a basic understanding of polymer conformational changes with process conditions.[11]

ES has drawn growing attention in fabricating fibers with diameters at the nano-/microscale because of its cost-effectiveness, simplicity, and versatility.[34–36] During the last few decades, ES has been successfully employed to produce fibers from a wide gamut of materials including plastics, block copolymers, blends, biopolymers, conducting polymers, composites, metal oxides, and ceramics.[37–39] The high surface-to-volume ratio provides enhanced material properties and endless possibilities to embed or coat functional moieties onto the fibers, rendering them useful in numerous potential applications from membrane technology to reinforced composites, enzyme immobilization, catalysis, tissue engineering, smart textiles, and functional coatings/sensors.[40–43]

Typically, a polymer solution or melt is extruded through a capillary tube (spinneret) to form a small droplet at the spinneret tip. The application of voltage between the tip of the spinneret and the collection plate generates surface charges in the polymer droplet, and when the applied voltage is above a critical value, the electrostatic forces overcome the surface tension in the polymer drop causing it to stretch to form a cone (referred to as Taylor cone) and eventually a liquid jet that is accelerated toward the grounded collection plate. During the flight of the resulting polymer jet, it experiences a combination of stretching and whipping due to bending instability (accompanied by solvent evaporation in polymer solutions), creating continuous ultrathin randomly oriented fibers in the form of a nonwoven mat deposited on a collecting plate. It is generally recognized that solution viscosity, surface tension, and electrical conductivity, among other parameters, greatly influence fiber formation (bead-free) and diameter.[44] It has been previously shown that adding ionic species to the solution increases its electrical conductivity. This allows a relatively higher surface charge density to be maintained on the ES jet and promote improved fiber extension during the whipping stage.[45] We investigated the effect of the incorporation of the Ag salt/NP on the three aforementioned polymer solution parameters and determined how they influenced fiber quality in terms of fiber diameter and bead formation.

2. Results and Discussion

Figure 1 is a schematic representing the procedure for the one-step synthesis of metal NP–PEO NF composites coupled with ES. Prior to forming electrospun NP–NF composites, we investigated the conditions and parameters by which AgNP

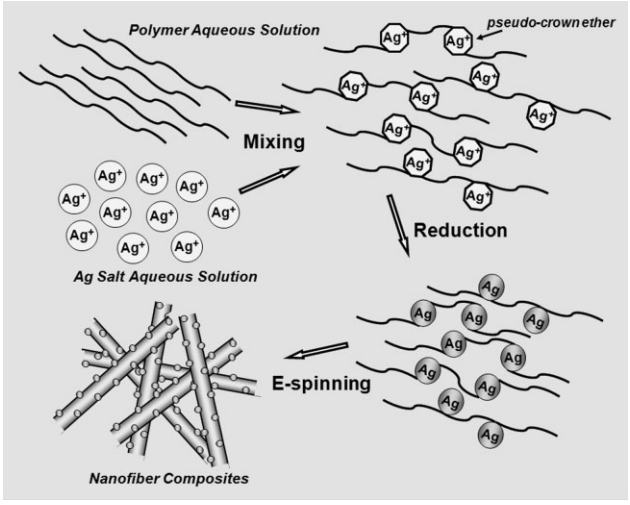

Figure 1. Schematic of the one-step process for fabricating metal NP–polymer NF composites via ES.

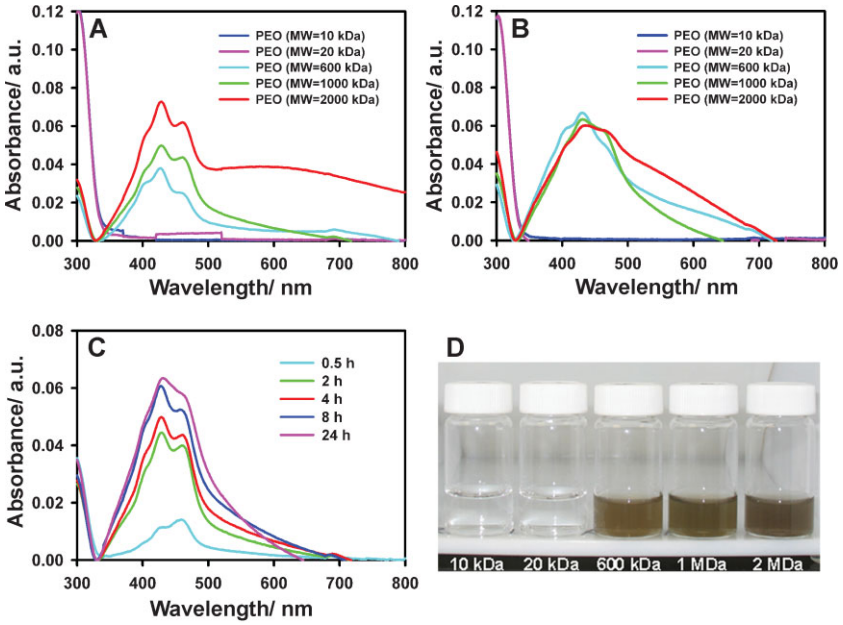

Figure 2. UV–Vis absorption spectra (A) 4 h and (B) 24 h after mixing $AgNO_3$ and PEO with different MWs (2 wt% PEO; 0.27 wt% $AgNO_3$)in H_2O at ambient conditions. C) Time evolution of the UV–Vis spectra of AgNPs prepared from $AgNO_3$ and PEO (1 MDa) in H_2O at ambient conditions (2 wt% PEO and 0.27 wt% $AgNO_3$). D) Picture of the aqueous solutions of $AgNO_3$ and PEO used in (A).

formation was achieved in solution with the electrospinning polymer, PEO as the in situ reductant. The in situ AgNP formation was monitored by UV–Vis absorption. It is generally accepted that the surface plasmon band resonance of AgNPs with sizes between 2–50 nm is observed in absorption in the UV–Vis spectrum at a wavelength in the range of 400–450 nm.[46,47] We found that there is absorption in this range for PEO with a MW of 600, 1000, and 2000 kDa, but not for PEO with a MW between 0.4 and 20 kDa at a concentration range of 0.06–0.36 wt% $AgNO_3$ and 2–4 wt% PEO (Figure 2A). It is also known that the magnitude of the absorption peak correlates to the concentration of AgNPs.[48,49] For all the reduction times tested (0.5, 1, 2, 4, 8, 24 h), the magnitude of the absorption peak in the UV–Vis absorption spectra obtained increased with the PEO MW. Figure 2A shows representative UV–Vis absorption spectra after 4 h of reduction of $AgNO_3$ and PEO with concentrations of 0.36 and 2 wt%, respectively. These data suggest that the rate of metal precursor reduction is MW-dependent where reduction is faster at higher MW, however, this dependency almost vanishes at the 24 h reduction time (Figure 2B). These results are consistent with the presumed mechanism of metal salt reduction via the formation of pseudo-crown ethers holding the metal cations within the coiled polyether helix. It has been shown that PEO fragments in PEO-containing copolymers are able to form pseudo-crown ether structures that can bind metal ions.[50–52] The reduction of bound metal ions can proceed via oxidation of PEO fragments by the metal center.[25] The reason for the similar conformation with that of the crown ethers is the ion–dipole interaction between the metal ion and the electron pair of the ether oxygen in the PEO fragments. The higher the PEO MW (or the longer the polymer chains are), the faster and the higher the number of crown ether cavities that can be formed, and therefore, the faster the reduction because of the higher number of reaction sites available.[53,54] The time evolution of the reduction process was also monitored by UV–Vis over the entire MW range (0.4, 6, 10, 20, 600, 1000, and 2000 kDa) and a representative spectrum is presented in Figure 2C. As early as 0.5 h after mixing the reactants, the onset of AgNP formation can be detected and the reaction is almost complete after 8 h. On the other hand, for PEO with a MW between 400 and 20 000 Da, even after 24 h no detection of AgNP formation was observed. This is consistent with a previous study using low MW (up to 20 kDa) PEO and a $AgNO_3$ metal precursor where it is reported that at least 20 days of reduction was required for AgNP formation to be detected.[25]

Aqueous solutions of high MW PEO and $AgNO_3$ were then used to fabricate NF composites of PEO and AgNPs by ES. The effect of incorporating AgNPs on NF diameter and bead formation during ES was also investigated. We determined that for 600 kDa PEO, NF formation is achieved and bead formation is at a minimum during ES at a concentration around 4 wt% and higher in H_2O. The same range of concentrations was reported by other groups as well.[55,56] AgNPs were then formed in 4 wt% 600 kDa PEO and up to 6 wt% $AgNO_3$ (based on the polymer that is equivalent to 0.26 wt% $AgNO_3$ in solution) and electrospun at a fixed solution flow rate of 1 mL h^{-1} and field strength of about 0.75 kV cm^{-1}. Changing the salt concentration at a fixed PEO amount enabled us to determine the effect of increasing $AgNO_3$ concentration on AgNP diameter.

Figure 3 provides the scanning electron microscopy (SEM; left column) and transmission electron microscopy (TEM; right column) images of the Ag NP–PEO NF mats fabricated from 4 wt% 600 kDa PEO and $AgNO_3$ (at concentrations from 0 to 0.26 wt%) aqueous solutions. The fiber size distribution for each NF mat was determined from at least 100 fibers from various SEM images and shows that the addition of AgNPs reduced the fiber diameter by at least 30% (from 313 nm for pure PEO to 214 ± 16 and 197 ± 21 nm, respectively) with the addition of 0.17 and 0.26 wt% $AgNO_3$ in the aqueous PEO solution. We anticipated that the addition of $AgNO_3$ to the PEO solution would have an effect (that is, decrease the fiber diameter) akin to the addition of inorganic salts such as NaCl even after the reduction of Ag^+ to neutral AgNPs. In a later section, we discuss the results of our investigation of electrospinning a PEO aqueous solution at a PEO concentration known to form beads but with the addition of AgNPs, bead formation is suppressed. This suppression is demonstrated to be related to the increase in solution conductivity concomitant to AgNP incorporation. We submit that this also

NANO MICRO small

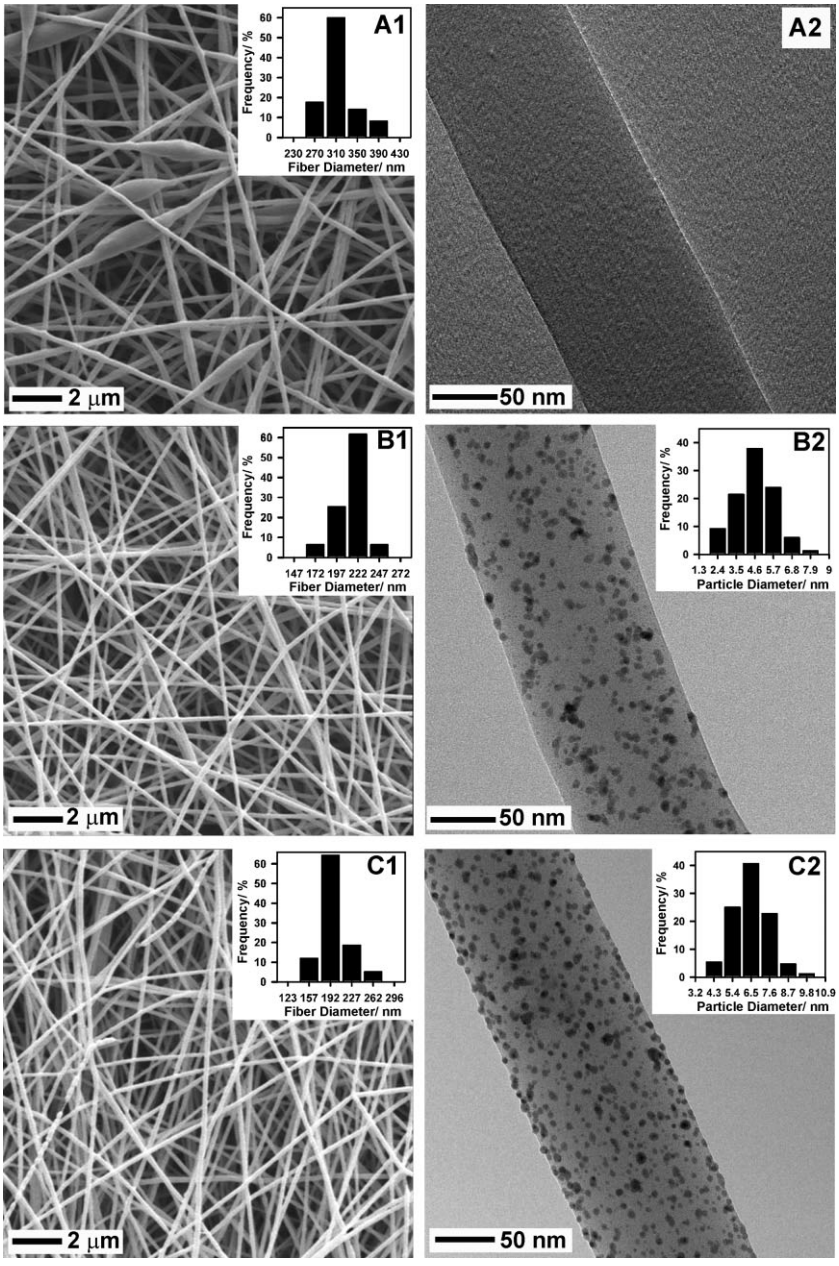

Figure 3. SEM (A1, B1, C1) and TEM (A2, B2, C2) images of the AgNP–PEO NF mats fabricated from aqueous solution of 4 wt% 600 kDa PEO and $AgNO_3$ at concentrations of (A) 0, (B) 0.17, and (C) 0.26 wt%.

explains the reduction in fiber diameter seen here. The average diameter of the AgNPs from the TEM images for the 0.12 and 0.18 wt% $AgNO_3$ is 4.6 ± 1.2 and 6.5 ± 1.1 nm, respectively. The increase in particle size is likely due to the increased incidence of coalescence of Ag atoms with higher Ag concentration.[4]

TEM micrographs of NFs from 2 wt% 2000 kDa PEO and 0.27 wt% $AgNO_3$ mixed in H_2O after 4 h are shown in Figure 4A and B. AgNPs are observed as dark spherical spots dispersed on the surface of the NF matrix with an average diameter of 8.1 ± 1.3 nm. From high resolution TEM (Figure 4B with inset) the crystalline structure of the particles is revealed by the presence of lattice fringes. The nanostructures are a mixture of single (continuous lattice fringes across the particle width) (inset of Figure 4B) and polycrystalline (multiply twinned) NPs (outset of Figure 4B). In one of the NPs imaged as shown in the inset of Figure 4B, the *d*-spacing was measured to be 0.235 nm, which corresponds to the (111) crystal plane of Ag.[57] The nature and crystallinity of the resulting AgNPs were further confirmed by X-ray diffraction (XRD) measurement for a corresponding Ag NP–NF mat (Figure 5A). The three XRD spectral peaks [(111), (200), and (311)] specific for elemental Ag were present.[58,59]

X-ray photoelectron spectroscopy (XPS) analyses were also performed on the same NF mat and the XPS data are shown in Figure 5B. The Ag $3d_{5/2}$ spectra of AgNP in the PEO NF matrix exhibited a single peak at a binding energy (BE) of 367.0 eV. It has been shown that the Ag $3d_{5/2}$ regions of the XPS spectra for Ag nanocomposite films are very vulnerable to the chemical environment surrounding the Ag species where it is shifted to lower BE when there is strong coordination.[60,61] Just recently, the Ag $3d_{5/2}$ spectra of AgNP (with $AgNO_3$ as the precursor) formed in situ after UV irradiation within an amphiphilic graft polymer containing ethylene oxide groups has been reported to be at a BE of 368.7 eV, whereas from pure $AgNO_3$ the BE is at 370.3 eV.[62] Furthermore, Wang et. al. measured the Ag $3d_{5/2}$ spectra of AgNP (in PVP NFs) formed by reduction of $AgNO_3$ by ethanol in PVP ethanol solution and also obtained a BE of 367.8 eV.[63] The lower BE obtained here with the PEO–$AgNO_3$ system (367.0 eV) is then likely due to the much stronger interaction between the resulting AgNPs and the ether oxygens of PEO. This stronger coordination/interaction also explains the spontaneous reduction of Ag^+ at ambient conditions. In comparison to PVP, reduction was not achieved at ambient conditions. As reported in the literature, heating is necessary to engender the reduction of $AgNO_3$ to form NPs.[10,24] The XPS data also distinguish the strength of interaction between the AgNP and the ether group of PEO on the basis of the MW. The BE of Ag $3d_{5/2}$ from ES composite fibers prepared from 4 wt% 600 kDa PEO (measured at 367.3 eV) is higher than that of 2000 kDa PEO (measured at 367.0 eV) and is much broader (Figure 3F inset). The full width at maximum height (FWMH) for 600 kDA PEO is 4.33 eV, while that of 2000 kDA PEO is 2.69 eV. Both peak shift and broadening has been previously determined to be related to the interaction of the Ag species with its chemical

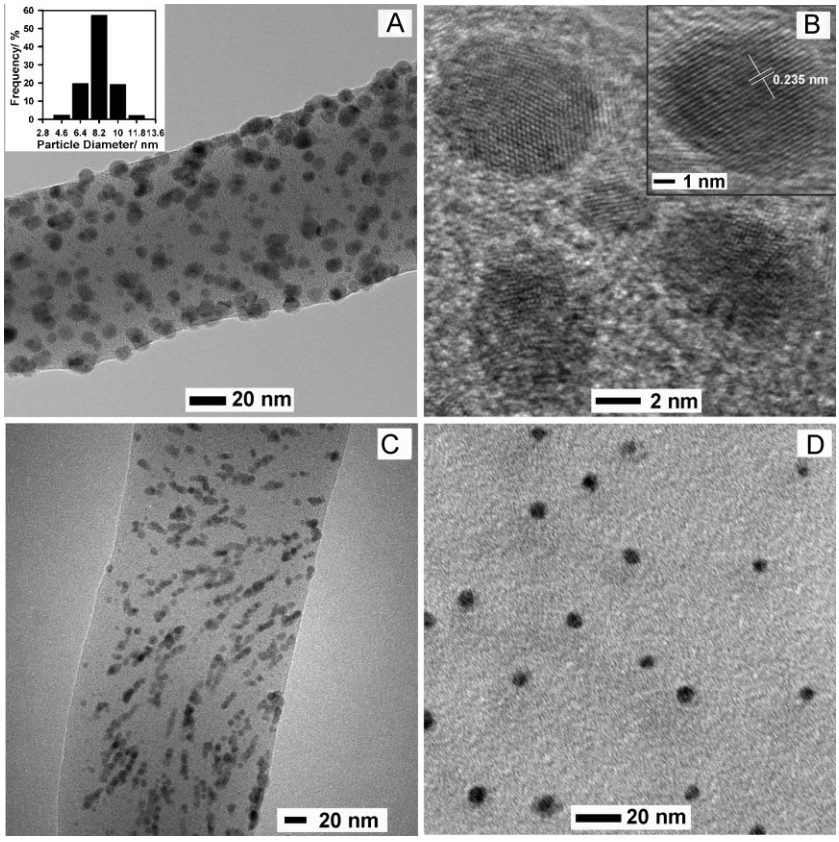

Figure 4. TEM images of ES NF mats from (A and B) a 2 wt% 2000 kDa PEO and 0.27 wt% of $AgNO_3$ aqueous solution after 4 h reduction and (C) a 4 wt% 600 kDa PEO and 0.26 wt% of $AgNO_3$ aqueous solution after 24 h reduction, and (D) a spin-coated film from the solution of (C).

environment.[64] The scenario that may be taking place during the in situ reduction is that there are more ether oxygen that are coordinating with the Ag species in the pseudo-crown formed with the higher MW PEO, hence the stronger interaction.

We found from the TEM images (e.g., Figure 4) that several of the AgNPs protrude in the surface of the NFs at higher Ag concentration. This may be due to the differentiated electrical field effects on the polymer and metal NPs having different electrical conductivity and polarizability. Another interesting phenomenon that was also observed is the localized alignment of NPs to form short nanochains in several of the NF composites (a representative TEM image is shown in Figure 4C). It has been shown that orientation of polarizable colloidal species can be spawned by the presence of an electrical field by inducing mobility and interaction between particles through a dielectrophoretic process.[65] In turn, the interactions between the dipoles induced in the particles can lead to formation of particle chains.[66] The alignment of NPs for the 600 kDa PEO was observed at the highest concentration of $AgNO_3$ tested here (0.26 wt%), indicating that proximity of NPs to each other maybe an important factor to the alignment. Lately, it has been reported that Cu–poly(vinyl alcohol) (PVA) nanocables were formed from PVA-protected CuNPs by ES. The authors speculated that the mechanism of the nanocable formation is related to the process described above and that the concentration of Cu plays a crucial role to the nanocable assembly. Interestingly, when the same Ag concentration was used with 2000 kDa PEO, no NP alignment or nanochain formation was observed (Figure 4A), signifying that viscosity (because of the higher MW) may also have substantial influence. We determined if such directed orientation could be the effect of surface energetics or inherent polymer solution properties and not induced by the applied electrical field. We prepared films of the same ES solution directly deposited into a TEM grid by spin-coating. Three films spin-coated separately on four TEM grids were prepared (with thickness of about 25 nm as measured by ellipsometry) and several frames of TEM images for each film were taken. In all of these no such orientation (alignment and protrusions) were observed in the absence of an electrical field as shown in the representative image in Figure 4D. It is also apparent that the NPs are less dense (far apart) compared to those of the ES nanocomposites and appear to be embedded randomly within the film. These results suggest that the applied electrical field can be used to modulate the spatial placement and orientation of NPs in the NFs. Further investigation is in progress to elucidate the mechanism of this NP orientation during ES.

To better understand the effect of AgNP incorporation using the proposed procedure, a solution at a 600 kDa PEO at a concentration where it is known to form beads upon ES was tested. At 3 wt% PEO aqueous solution, different concentrations from 1 to 20 wt% $AgNO_3$ based on the PEO content were electrospun and it was found that at 2 wt% $AgNO_3$, bead formation was dramatically reduced (Figure 6). Bead formation is known to be related to viscosity, electrical conductivity (EC), and surface tension of the ES solution.[44] To identify which among these solution parameters explain the dramatic reduction in bead formation as well as in fiber diameter, the solution viscosity, electrical conductivity, and surface tension were measured using a rheometer (TA Instruments), EC meter (Fisher Accumet BASIC AB30), and an oscillating pendent drop tensiometer (TRACKER) from IT Concept (used as described in Yang et al.[67]), respectively, for the pure 3 wt% PEO solution and the PEO solution with 0.03 to 0.06 wt% $AgNO_3$. These solution parameters are well known to have a substantial effect on NF quality. The results as provided in Table 1 indicate that the reduction in bead formation as well as in fiber diameter upon the incorporation of AgNPs is due to the almost seven-fold increase in the EC of the solution. This increase in the EC leads to the enhancement of the electrical charge density in the solution, causing stronger elongation forces in the ejected jets within the electrical field

small NANO MICRO

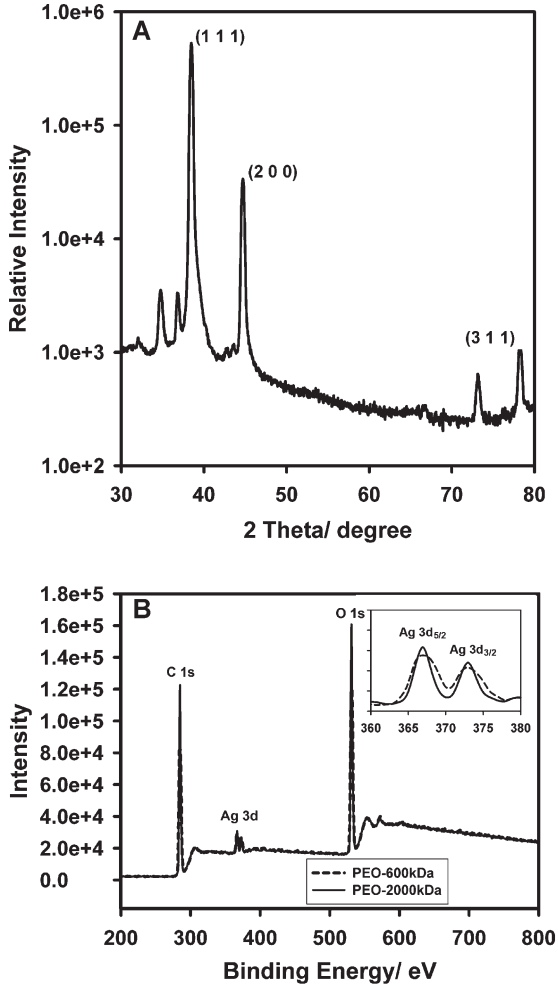

Figure 5. A) XRD and B) XPS spectra of ES NF mats from a 2 wt% 2000 kDa PEO and 0.27 wt% of $AgNO_3$ aqueous solution after 4 h reduction. XPS spectra of an ES NF mat from a 2 wt% 600 kDa PEO and a 0.27 wt% $AgNO_3$ aqueous solution are also included in B.

upon the application of voltage during ES. Interestingly, at 0.03 wt% $AgNO_3$ concentration, where the conductivity increased by at least a factor of three, bead formation is still extensive (Figure 6B), indicating that there is a minimum magnitude of conductivity necessary for fiber formation. On the other hand, at 0.3 wt% $AgNO_3$ concentration, a discontinuous fiber mat (broken fibers as shown in Figure 6D) is achieved, which may be due to excessive elongation forces with the concomitant tremendous increase in the solution conductivity (Table 1). Recently, it was shown by Thompson et al. by using theoretical treatment of the ES process that indeed electrical charge density has a primary effect on NF formation and the resulting NF diameter.[68]

3. Conclusions

This study has described a successful genuine one-step fabrication of Ag NP–PEO NF composites via a green ES at ambient conditions. The novelty of the methodology lies on the use of the ES polymer as the reducing agent for the metal salt precursor and at the same time as the protecting and templating agent for the resulting NPs. This procedure circumvents the necessity of separately synthesizing and isolating uniform and stabilized colloids in solution to combine with the ES polymer. Moreover, it eliminates the need of using conventional chemical, thermal, or radiolytic reduction treatments and the addition of protecting agents. The NPs are a mixture of single- and polycrystalline spherical particles dispersed on the surface of the NFs. The incorporation of AgNPs in the ES solution tremendously improves the fiber quality through reduction in fiber diameter and in bead formation. This fiber quality improvement is attributable to the increased EC in the ES solution upon the incorporation of NPs.

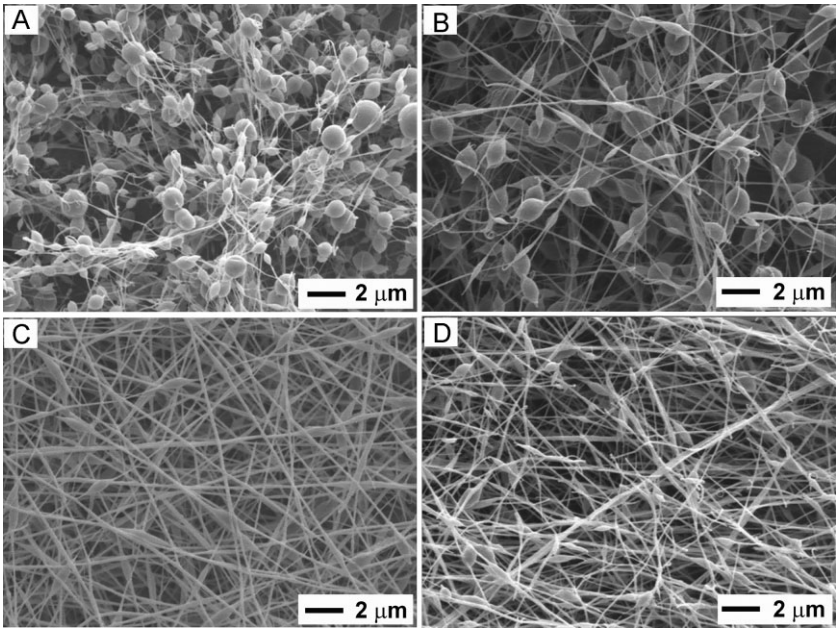

Figure 6. SEM images of Ag NP–PEO NF mats fabricated from 3 wt% 600 kDa PEO and (A) 0, (B), 0.03, (C) 0.06, and (D) 0.3 wt% $AgNO_3$ concentration in aqueous solution.

4. Experimental Section

For a typical procedure, predetermined amounts of PEO (Polysciences, MW = 600–2000 kDa) and $AgNO_3$ (Fisher, 99%) are dissolved in deionized water (d-H_2O) in two separate vials. The PEO mixture is left to stir for 3 to 4 h to ensure complete dissolution, after which the two solutions are combined to effect the reduction of the metal salt precursor by PEO at ambient conditions in sealed vials. After the reduction, the solution is left for an hour to eliminate the air bubbles and is subsequently electrospun. The ES apparatus includes a precision syringe pump (Harvard Apparatus, Holliston, MA), which is operated at a flow rate of 0.1–99 mL h^{-1}, and a high-voltage power supply (Gamma High Voltage Research, model D-ES30 PN/M692 with a positive polarity). The operating voltage was varied from 0 to 30 kV with an optimum

Table 1. Measured $AgNO_3$–PEO solution parameters at ambient conditions.

Solution wt% $AgNO_3$ in 3 wt% aqueous PEO	Viscosity [Pa s]	Electrical Conductivity [μS]	Surface Tension [dyne cm^{-1}]
0	6.0	91.2	54.2 ± 0.4
0.03	6.3	353.3	54.5 ± 0.4
0.06	6.5	705.0	54.9 ± 0.5
0.3	–	2365.0	–

electric field of 1 kV cm^{-1}. The solutions were loaded into 10 mL syringes with Luer-lock connections and used in conjunction with a 2 in. 22-gauge blunt tip needle. The design of the ES setup was based on a point-plate configuration, where the ES fiber mats were deposited onto Al foil placed over a steel collector plate. The morphology and size of the resulting ES nonwoven fiber mats were evaluated using SEM (FEI XL30). The incorporated metal NPs were characterized using TEM (Hitachi HF-2000), XPS (Kratos Analytical Axis Ultra), and XRD (Philips X'Pert PRO MRD HR XRD System). Samples for analyses were removed from the collector plate including TEM samples where they were deposited directly to TEM carbon-coated copper grids (Electron Microscopy Sciences) fastened to the Al foil. The reduction and NP formation by PEO in aqueous solution, along with the time evolution of the reduction process, were monitored by UV–Vis absorbance spectrophotometry (Jasco V550).

Acknowledgements

This work was supported by the STC program of the US National Science Foundation under agreement (CHE-9876674). The authors thank Dr. Vincent J. Verruto for his assistance with the surface tension measurements.

[1] B. F. G. Johnson, *Coord. Chem. Rev.* **1999**, *192*, 1269–1285.
[2] J. D. Aiken, R. G. Finke, *J. Mol. Catal. A* **1999**, *145*, 1–44.
[3] C. B. Murray, C. R. Kagan, M. G. Bawendi, *Annu. Rev. Mater. Sci.* **2000**, *30*, 545–610.
[4] C. D. Saquing, T. T. Cheng, M. Aindow, C. Erkey, *J. Phys. Chem. B* **2004**, *108*, 7716–7722.
[5] C. D. Saquing, D. Kang, M. Aindow, C. Erkey, *Microporous Mesoporous Mater.* **2005**, *80*, 11–23.
[6] A. Y. Stakheev, L. M. Kustov, *Appl. Catal. A* **1999**, *188*, 3–35.
[7] J. Ramos, A. Millan, F. Palacio, *Polymer* **2000**, *41*, 8461–8464.
[8] C. Castro, J. Ramos, A. Millan, J. Gonzalez-Calbet, F. Palacio, *Chem. Mater.* **2000**, *12*, 3681–3688.
[9] L. L. Beecroft, C. K. Ober, *Chem. Mater.* **1997**, *9*, 1302–1317.
[10] Y. J. Xiong, I. Washio, J. Y. Chen, H. G. Cai, Z. Y. Li, Y. N. Xia, *Langmuir* **2006**, *22*, 8563–8570.
[11] G. M. Kim, A. Wutzler, H. J. Radusch, G. H. Michler, P. Simon, R. A. Sperling, W. J. Parak, *Chem. Mater.* **2005**, *17*, 4949–4957.
[12] W. K. Son, J. H. Youk, T. S. Lee, W. H. Park, *Macromol. Rapid Commun.* **2004**, *25*, 1632–1637.
[13] J. Bai, Y. Li, S. Yang, J. Du, S. Wang, J. Zheng, Y. Wang, Q. Yang, X. Chen, X. Jing, *Solid State Commun.* **2007**, *141*, 292–295.
[14] X. Xu, Q. Yang, Y. Wang, H. Yu, X. Chen, X. Jing, *Eur. Polym. J.* **2006**, *42*, 2081–2087.
[15] D. I. Gittins, F. Caruso, *Angew. Chem. Int. Ed.* **2001**, *40*, 3001–3004.
[16] C. J. Kiely, J. Fink, J. G. Zheng, M. Brust, D. Bethell, D. J. Schiffrin, *Adv. Mater.* **2000**, *12*, 640–643.
[17] M. Jin, X. Zhang, S. Nishimoto, Z. Liu, D. A. Tryk, T. Murakami, A. Fujishima, *Nanotechnology* **2007**, *18*, 075605.
[18] A. C. Patel, S. Li, C. Wang, W. Zhang, Y. Wei, *Chem. Mater.* **2007**, *19*, 1231–1238.
[19] Z. Y. Li, H. M. Huang, T. C. Shang, F. Yang, W. Zheng, C. Wang, S. K. Manohar, *Nanotechnology* **2006**, *17*, 917–920.
[20] Y. Z. Wang, Q. B. Yang, G. Y. Shan, C. Wang, J. S. Du, S. G. Wang, Y. X. Li, X. S. Chen, X. B. Jing, Y. Wei, *Mater. Lett.* **2005**, *59*, 3046–3049.
[21] W. J. Jin, H. K. Lee, E. H. Jeong, W. H. Park, J. H. Youk, *Macromol. Rapid Commun.* **2005**, *26*, 1903–1907.
[22] B. H. Hong, S. C. Bae, C. W. Lee, S. Jeong, K. S. Kim, *Science* **2001**, *294*, 348–351.
[23] I. Washio, Y. Xiong, Y. Yin, Y. Xia, *Adv. Mater.* **2006**, *18*, 1745–1749.
[24] C. E. Hoppe, M. Lazzari, I. Pardinas-Blanco, M. A. Lopez-Quintela, *Langmuir* **2006**, *22*, 7027–7034.
[25] L. Longenberger, G. Mills, *J. Phys. Chem. B* **1995**, *99*, 475–478.
[26] T. Sakai, P. Alexandridis, *J. Phys. Chem. B* **2005**, *109*, 7766–7777.
[27] A. M. Christie, S. J. Lilley, E. Staunton, Y. G. Andreev, P. G. Bruce, *Nature* **2005**, *433*, 50–53.
[28] B. Duan, C. H. Dong, X. Y. Yuan, K. D. Yao, *J. Biomater. Sci. Polym. Ed.* **2004**, *15*, 797–811.
[29] J. Zeng, X. Xu, X. Chen, Q. Liang, X. Bian, L. Yang, X. Jing, *J. Controlled Release* **2003**, *92*, 227–231.
[30] E. R. Kenawy, G. L. Bowlin, K. Mansfield, J. Layman, D. G. Simpson, E. H. Sanders, G. E. Wnek, *J. Controlled Release* **2002**, *81*, 57–64.
[31] S. Hirano, M. Zhang, M. Nakagawa, T. Miyata, *Biomaterials* **2000**, *21*, 997–1003.
[32] X. H. Qin, Y. Q. Wan, J. H. He, J. Zhang, J. Y. Yu, S. Y. Wang, *Polymer* **2004**, *45*, 6409–6413.
[33] A. G. MacDiarmid, W. E. Jones, I. D. Norris, J. Gao, A. T. Johnson, N. J. Pinto, J. Hone, B. Han, F. K. Ko, H. Okuzaki, M. Llaguno, *Synth. Met.* **2001**, *119*, 27–30.
[34] S. V. Fridrikh, J. H. Yu, M. P. Brenner, G. C. Rutledge, *Phys. Rev. Lett.* **2003**, *90*, 144502.
[35] D. Li, G. Ouyang, J. T. McCann, Y. N. Xia, *Nano Lett.* **2005**, *5*, 913–916.
[36] X. Y. Sun, R. Shankar, H. G. Borner, T. K. Ghosh, R. J. Spontak, *Adv. Mater.* **2007**, *19*, 87–91.
[37] D. Li, Y. L. Wang, Y. N. Xia, *Nano Lett.* **2003**, *3*, 1167–1171.
[38] Q. Peng, X. Y. Sun, J. C. Spagnola, G. K. Hyde, R. J. Spontak, G. N. Parsons, *Nano Lett.* **2007**, *7*, 719–722.
[39] D. Li, Y. N. Xia, *Nano Lett.* **2003**, *3*, 555–560.
[40] C. Drew, X. Liu, D. Ziegler, X. Y. Wang, F. F. Bruno, J. Whitten, L. A. Samuelson, J. Kumar, *Nano Lett.* **2003**, *3*, 143–147.
[41] Z. M. Huang, Y. Z. Zhang, M. Kotaki, S. Ramakrishna, *Compos. Sci. Technol.* **2003**, *63*, 2223–2253.
[42] D. H. Reneker, I. Chun, *Nanotechnology* **1996**, *7*, 216–223.
[43] D. Li, Y. N. Xia, *Adv. Mater.* **2004**, *16*, 1151–1170.
[44] H. Fong, I. Chun, D. H. Reneker, *Polymer* **1999**, *40*, 4585–4592.

[45] B. Kim, H. Park, S. H. Lee, W. M. Sigmund, *Mater. Lett.* **2005**, *59*, 829–832.
[46] A. Moores, F. Goettmann, *New J. Chem.* **2006**, *30*, 1121–1132.
[47] S. G. Boyes, B. Akgun, W. J. Brittain, M. D. Foster, *Macromolecules* **2003**, *36*, 9539–9548.
[48] D. B. Zhang, L. M. Qi, J. M. Ma, H. M. Cheng, *Chem. Mater.* **2001**, *13*, 2753–2755.
[49] L. M. Liz-Marzan, I. Lado-Touriño, *Langmuir* **1996**, *12*, 3585–3589.
[50] A. Warshawsky, R. Kalir, A. Deshe, H. Berkovitz, A. Patchornik, *J. Am. Chem. Soc.* **1979**, *101*, 4249–4258.
[51] M. D. Adams, P. W. Wade, R. D. Hancock, *Talanta* **1990**, *37*, 875–883.
[52] K.-J. Liu, *Macromolecules* **1968**, *1*, 308–311.
[53] S. Yanagida, K. Takahashi, M. Okahara, *Bull. Chem. Soc. Jpn.* **1977**, *50*, 1386–1390.
[54] F. E. Bailey, J. V. Koleske, *Alkylene Oxides and their Polymers*, Marcel Dekker, New York 1991.
[55] M. Gensheimer, M. Becker, A. Brandis-Heep, J. H. Wendorff, R. K. Thauer, A. Greiner, *Adv. Mater.* **2007**, *19*, 2480–2482.
[56] C. Wang, E. Y. Yan, Z. Y. Sun, Z. J. Jiang, Y. B. Tong, Y. Xin, Z. H. Huang, *Macromol. Mater. Eng.* **2007**, *292*, 949–955.
[57] International Center for Diffraction Data file #03-0931 for FCC silver metal.
[58] D. G. Yu, W. C. Lin, C. H. Lin, L. M. Chang, M. C. Yang, *Mater. Chem. Phys.* **2007**, *101*, 93–98.
[59] X. C. Jiang, Y. Xie, J. Lu, L. Y. Zhu, W. He, Y. T. Qian, *Langmuir* **2001**, *17*, 3795–3799.
[60] J. H. Kim, B. R. Min, J. Won, S. H. Joo, H. S. Kim, Y. S. Kang, *Macromolecules* **2003**, *36*, 6183–6188.
[61] Y. Kobayashi, V. Salgueirino-Maceira, L. M. Liz-Marzan, *Chem. Mater.* **2001**, *13*, 1630–1633.
[62] Y. W. Kim, D. K. Lee, K. J. Lee, B. R. Min, J. H. Kim, *J. Polym. Sci, Part B: Polym. Phys.* **2007**, *45*, 1283–1290.
[63] Y. Z. Wang, Y. X. Li, S. T. Yang, G. L. Zhang, D. M. An, C. Wang, Q. B. Yang, X. S. Chen, X. B. Jing, Y. Wei, *Nanotechnology* **2006**, *17*, 3304–3307.
[64] J. F. Weaver, G. B. Hoflund, *Chem. Mater.* **1994**, *6*, 1693–1699.
[65] S. Gangwal, O. J. Cayre, M. Z. Bazant, O. D. Velev, *Phys. Rev. Lett.* **2008**, *100*, 058302.
[66] S. Gupta, R. G. Alargova, P. K. Kilpatrick, O. D. Velev, *Soft Matter* **2008**, *4*, 726–730.
[67] X. L. Yang, V. J. Verruto, P. K. Kilpatrick, *Energy Fuels* **2007**, *21*, 1343–1349.
[68] C. J. Thompson, G. G. Chase, A. L. Yarin, D. H. Reneker, *Polymer* **2007**, *48*, 6913–6922.

Received: September 1, 2008
Revised: December 22, 2008
Published online: March 12, 2009

